Anno 2011_Numero 188

rapporti tecnici INGV

The InfraCyrus infrasound sensor

188

Istituto Nazionale di Geofisica e Vulcanologia

Segreteria di Redazione
Francesca Di Stefano - coordinatore
Tel. +39 06 51860068
Fax +39 06 36915617
Rossella Celi
Tel. +39 06 51860055
Fax +39 06 36915617

redazionecen@ingv.it

ISSN 2039-7941
Anno 2011_Numero 188

rapporti tecnici

INGV

THE INFRACYRUS INFRASOUND SENSOR

Ciro Buonocunto, Luca D'Auria, Antonio Caputo, Marcello Martini, Massimo Orazi

INGV (Istituto Nazionale di Geofisica e Vulcanologia, Sezione di Napoli - Osservatorio Vesuviano)

188

Table of contents

Introduction

Infrasound sensors are used for a wide range of geophysical applications as the monitoring of volcanic eruptions, the detection of bolides and the recording of infrasounds generated by earthquakes. In 2006 we started the development of cheap infrasound sensors, based on commercial electret microphones. They have been characterized by comparing their response function with existing broadband infrasound sensors. These sensors, called *InfraCyrus*, have a good response between 1 and 10 Hz, making their application useful for various geophysical purposes. Currently, about a dozen of sensors are deployed in the Neapolitan area showing good performances in the recording of local and regional infrasonic transients.

1. Low frequency response of electret microphones

Electret condenser microphones (ECM) consist in a membrane made of a dielectric material polarized with a permanent electrostatic charge [Sessler 1987]. Pressure transients acting on the membrane cause slight changes in the electret capacity. Because of the constant electrostatic charge, this turns in a variation in the output voltage of the electret. Because of the low output level and the high impedance of the source, it is usually connected to a high impedance FET preamplier (Fig. 1). Compared with conventional condenser microphones, they do not require an external polarizing voltage.

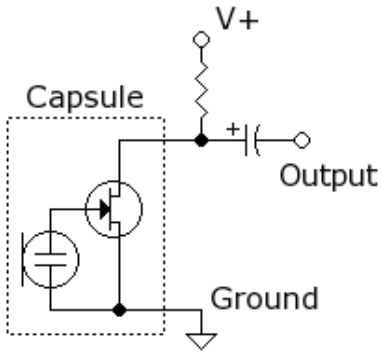

Figure 1. Simplified scheme of an ECM. The capsule contains both the electret and a FET preamplifier.

We have checked the feasibility of developing infrasound sensors based on Panasonic WM034DM ECMs which are widely used. In Table 1 we summarize the characteristics of these ECMs.

A preliminary task was to quickly check the quality of a set of about 30 WM034DM ECMs in order to verify their response at frequencies around 1 Hz. The datasheet shows a response only from 20 Hz, so we have developed an experimental apparatus to test their response at frequencies between 0.05 and 100 Hz (Fig. 2). The source of low frequency vibrations consists of a commercial closed-box sub-woofer (Fig. 3) driven by a low distortion wide range amplifier having as input a sinusoidal signal. The subwoofer enclosure is acoustically coupled with the ECM through a 1 m long plastic hose (Fig. 3). During the test the ECMs are located at the hose outlet. The output voltages were amplified by a factor 4 and the peak-to-peak amplitudes were measured using an oscilloscope (Fig. 2). In Figure 4 we show an histogram with the statistics of output values for 30 ECMs for an input sinusoid with a frequency of 1 Hz. The output values span the interval 0.8-2.2 V for the same input.

Results of this test demonstrate that commercial ECMs can have a good response even at low frequencies, below the 20 Hz limit. However since their characteristics are no more documented and seem to show a significant degree of variability, they need to be carefully calibrated.

Parameter	Value
Sensitivity	1 V/Pa at 1 kHz
Impedance	<2.2 kΩ
Directivity	Omnidirectional
Frequency	20÷16000 Hz
Max. operation voltage	10 V
Standard operation voltage	1.5 V
Current consumption	Max 0.3 mA
S/N ratio	>60 dB

Table 1. Specification of the WM-034DM ECM [see URL in references for the complete datasheet].

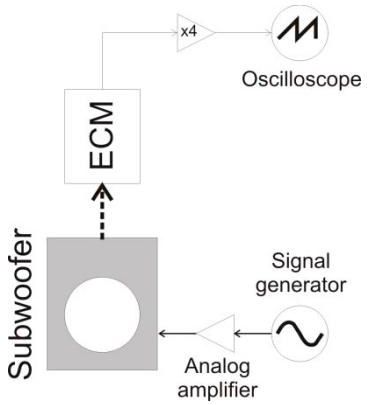

Figure 2. Scheme of the apparatus for testing ECMs.

Figure 3. Picture of the subwoofer used for the tests. Note the plastic hose connected with the enclosure.

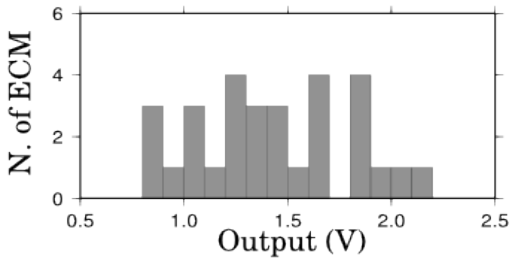

Figure 4. Histogram with the output voltage resulting from the testing of 30 ECMs. The bin width is 0.1 V.

2. Electronics and packaging of the *InfraCyrus* sensor

The electret output is connected to an electronic conditioning unit which is needed to amplify and filter the signals, in order to make the sensor output compatible with typical requirements of digital acquisition systems. It consists of a low noise amplifier, followed by a low-pass filter (Fig. 5). The ECM is polarized through a 10 kΩ resistor and its output is decoupled using a simple RC filter with a cut-off frequency of about 0.07 Hz. The first stage of the circuit is a low noise operational amplifier in non-inverting configuration. Its gain can be changed by setting, through jumpers placed on the circuit board, the value of the resistor R_k (see Fig. 5). This allows to set the gain to the following values: 4, 8, 12 or 16. The second stage consists of a low-pass second order Butterworth filter with a cut-off frequency of 50 Hz. We have not used electrolytic condensers, on the signal path, to avoid an excessive signal leak, typical of these components. The frequency response of the conditioning unit is shown in Figure 6. It is flat within ±3dB between 0.07 and 50 Hz. This experimental curve has been obtained using a sinusoidal input.

The dual power voltage needed for op-amps (±12 V) is obtained using a DC/DC converter (TRACO mod. TEN 3 1222) which allows the use of a wide range of input voltage (9-18 V). This choice was motivated by considering that often field installations are powered by solar panels and batteries whose voltage levels (12 V) are poorly stable.

The output has a low impedance (about 100 Ω), making the sensor capable to drive long lines with only a minor signal attenuation. This allows field installations with the sensors located tens of meters away from the digital data acquisition system(e.g. infrasonic arrays).

Circuit boards (Fig. 7) have been realized on single sides PCB fiber glass. Each board, with the ECM and a mechanical filter, is enclosed in a sealed PVC container (IP65 protection rating), with dimensions 10x10x5 cm (Fig. 8). This type of container, is well suited for volcanic environments, where corrosion phenomena are likely to occur on metal enclosures. We have also added a polyurethane closed-cell foam mechanical filter. This filter surrounds the ECM and it has been shown to be efficient in reducing wind induced noise [Shams et al., 2005]. The coupling of the acoustic inlet (Fig. 8) has been realized with a microporous garden hose with a length of 2-3 m. This is also a valid tool to further reduce the wind noise [Walker and Hedlin, 2009].

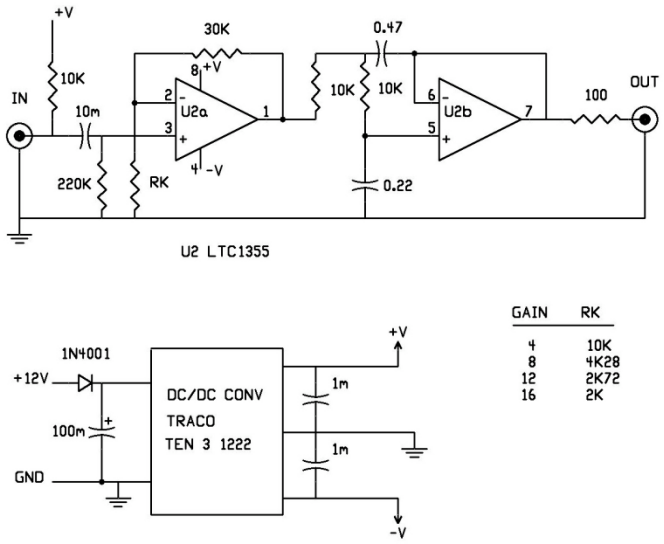

Figure 5. Electrical diagram of the conditioning unit of the *InfraCyrus* sensor. On the top there is the conditioning circuit, while on the bottom there is the DC/DC unit. The table on the right indicates the relationship between R_k and the output gain.

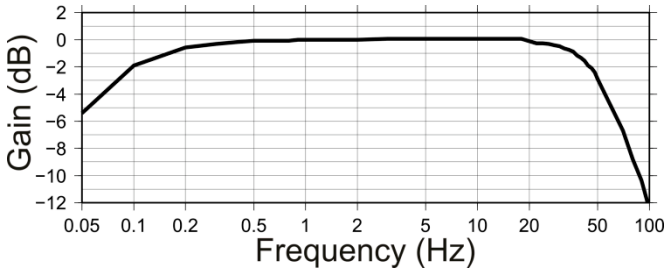

Figure 6. Frequency response of the whole electronic conditioning circuit.

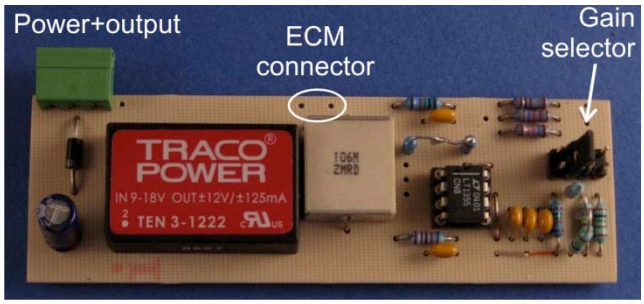

Figure 7. Annotated picture of the *InfraCyrus* sensor electronic board.

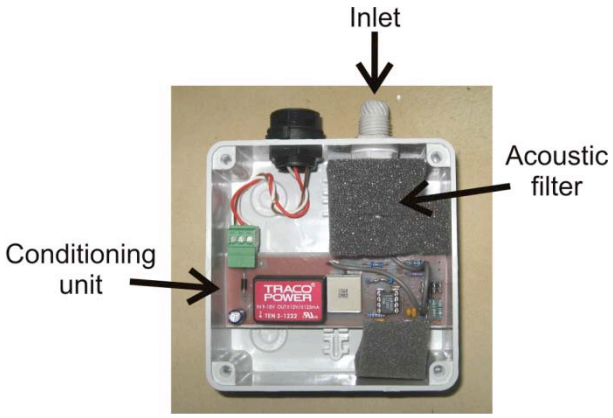

Figure 8. Annotated picture of the *InfraCyrus* sensor enclosure.

3. Relative calibration of the sensors

The full characterization of the *InfraCyrus sensor* response has been obtained by using a relative comparison with a *Chaparral 25V* infrasound sensor [*Model 25V*], see URL in References for the complete datasheet]. The response function of this sensor is known from its datasheet; we denote it as $R_{25V}(\omega)$. Giving the same input to both sensors we get two outputs: $O_{25V}(\omega)$ and $O_{IC}(\omega)$. Then the response function of the *InfraCyrus* sensor can be written as: $R_{IC}(\omega)= R_{25V}(\omega)*[O_{IC}(\omega)/ O_{25V}(\omega)]$. In practice the value of $R_{IC}(\omega)$ is computed only at a set of 15 discrete frequencies, from 0.1 Hz up to 70 Hz.

The experimental apparatus basically consists of a subwoofer coupled directly with the *Chaparral* sensor and with two *InfraCyrus* sensors to be tested (Fig. 9). The outputs of the sensors, together with the signal generator input are digitized using a 4-channel 24bit GILDA digitizer [Orazi et al., 2006] (Fig. 9). The maximum length of the hoses is about 1 m. This size is short enough to prevent significant propagation effects even at the highest frequency used in the calibration procedure (the wavelength of sound at 70 Hz is about 5 m).

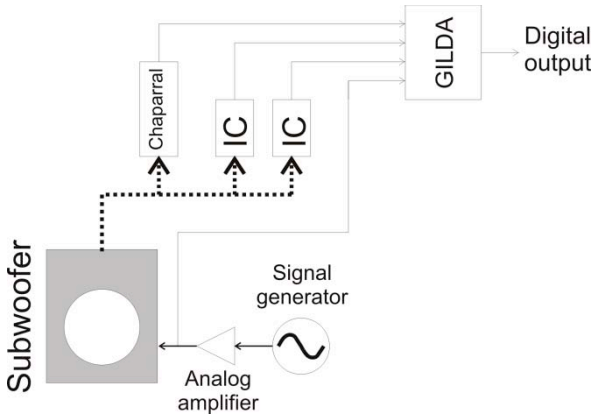

Figure 9. Scheme of the apparatus for the calibration of the *InfraCyrus* sensor. Chaparral indicates the *Chaparral 25V* sensor, while IC indicates the *InfraCyrus* sensors.

In Figure 10, we compare the outputs of two *InfraCyrus* sensors in the experimental setting of Figure 9. The input signals consists of a set of sinusoids with progressively decreasing frequencies (70, 50, 30, 20, 10, 7, 5, 3, 2, 1, 0.7, 0.5, 0.3, 0.2, 0.1 Hz). Each frequency has been recorded for an interval long enough to contain at least 10 cycles.

We observe how at high frequencies, the *InfraCyrus* sensor response is excellent compared with the broadband sensor. It should be remarked that during this procedure, the *Chaparral* sensor sensitivity has been set to 0.05 V/Pa (it can also be set to 0.5 V/Pa). Anyway it can also be seen how, at lower frequencies, the amplitude of the *InfraCyrus* sensor signal decays more rapidly than the *Chaparral*. In Figure 11 we represent the result of the relative calibration of one of the *InfraCyrus* sensors. The symbols (circles and crosses) indicates the experimental values. A simple linear system, with one zero at the origin and two poles on the negative side of the real axis, fits satisfactorily the experimental values (Fig. 11). The position of the two poles is determined, for each sensor, by a simple trial and error approach. In Figure 12 we represent the position of poles and zeroes for the dashed curves shown in Figure 11.

We observe that the response of different *InfraCyrus* sensors shows a limited degree of variability (Fig. 13). All the sensor show a nearly flat response between 1 and 10 Hz. Their sensitivity at 1 Hz is between 0.125 and 0.2 V/Pa. Our experimental apparatus was not able to determine the full dynamical range of the sensor. We have tested signals only up to 10 Pa.

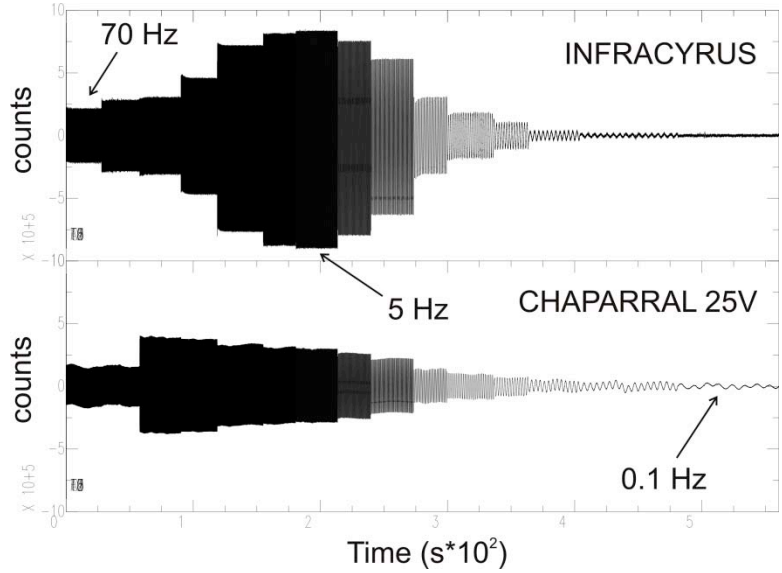

Figure 10. Comparison of the output of the two sensors. The vertical scale is the same.

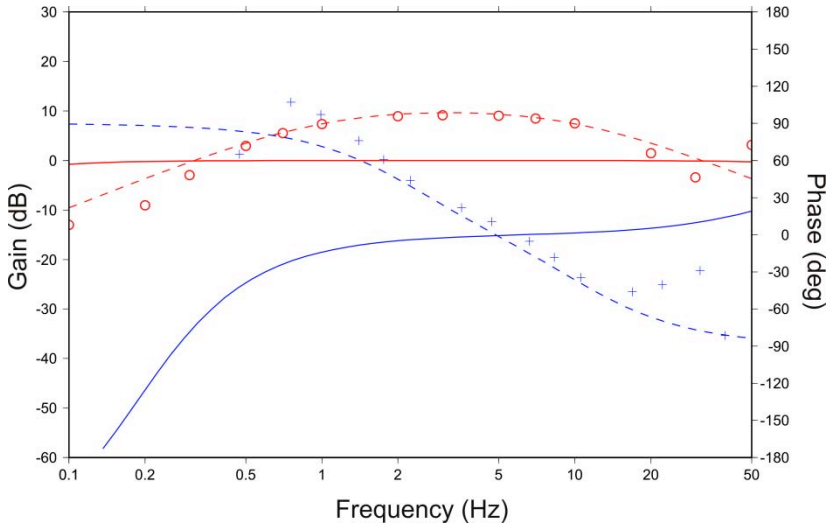

Figure 11. Response function of the *InfraCyrus* sensor (dashed lines) plotted together with the response of the *Chaparral* sensor (solid lines). Red lines represents the gain, while blue lines the phase. Circles and crosses are the experimental data (see text for details).

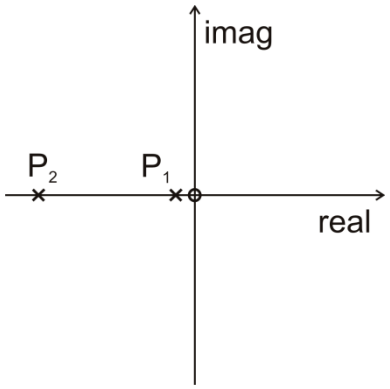

Figure 12. Poles and zeros of the *InfraCyrus* sensor response function in Figure 11. There is one zero at the origin. The two poles are P_1=(-6.3,0) and P_2=(-63.0,0).

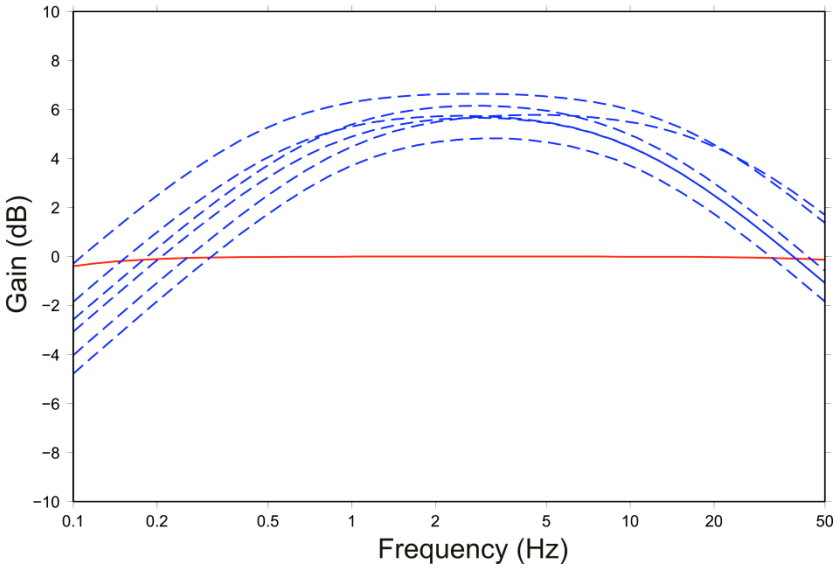

Figure 13. Comparison of the gain of 6 *InfraCyrus* sensors (blue dashed curves) with the response of *Chaparral* sensor (solid red curve).

4. Example recordings

The *InfraCyrus* sensors, are part of a research project, led by INGV-Osservatorio Vesuviano, aimed at the development of a regional infrasound monitoring network. The project aims are the infrasonic monitoring of volcanic activity and the discrimination between natural (ex. volcanic explosions, earthquakes, thunders, bolides) and artificial sources (ex. artificial explosion). Furthermore the observation in 2005 of a powerful seismo-acoustic transient related to a bolide airburst close to Ischia island [D'Auria etal., 2006], opened new research perspectives in this field. Up to now, about 12 *InfraCyrus* sensors have been deployed on the field: 6 on Vesuvius, 4 on Campi Flegrei and 2 on Ischia. Procedures for the real-time automatic detection and analysis of infrasonic transients are under development.
Since 2006 *InfraCyrus* sensors on the field have recorded a wide range of signals both on a local scale (artificial explosions, thunders, sonic booms, airplane and helicopters) and on a regional scale. In Figure 14 we represent a typical recording at station CSFT (Solfatara crater) of an artificial explosion located (on the basis of seismic traveltimes) within the Pozzuoli Bay. It can be seen how the infrasonic signal consists of two distinct phases. The first resembles the envelope of the seismic component and it is related to the seismo-acoustic conversion at the surface [Arrowsmith et al., 2010]. The second phase is the proper infrasonic phase, arriving with a delay of about 14 s, corresponding to a distance of 4.5 km. This estimate is consistent with the source-station distance.

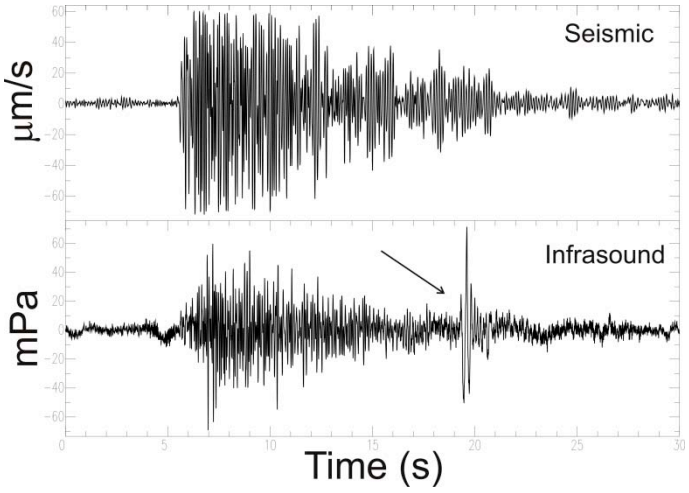

Figure 14. The upper signal is the seismic recording (vertical component) of an artificial explosion in the Pozzuoli Bay. The lower is the infrasound recorded on the same site (station CSFT, Solfatara). The sampling rate is 100 Hz for both signals.

The propagation of infrasounds on a regional scale is strongly affected by the complex velocity structure of the upper atmosphere and by the effect of the wind pattern [Evers and Haak, 2009]. Since 2006 we have recorded various events showing a dispersed waveform typical of a regional propagation. One event was linked to a huge blast of a military ammunition depot occurred on 15 March 2008 in Gërdec (Albania). Other events were linked to strong explosions of Stromboli volcano. In Figure 15 we show the recording (again at station CSFT) of the Gërdec explosion and of a powerful Vulcanian explosion occurred at Stromboli volcano during the 2007 effusive eruption [Martini et al., 2007].

Conclusions

We have designed, developed and tested an infrasound sensor based on low cost commercial components. It shows a good response between about 0.07 and 50 Hz, making it suitable for the purposes of infrasound monitoring [Evers, 2009]. The sensors, currently operating on the Neapolitan volcanoes, have already shown interesting results and have delineated future potential applications which are under development.

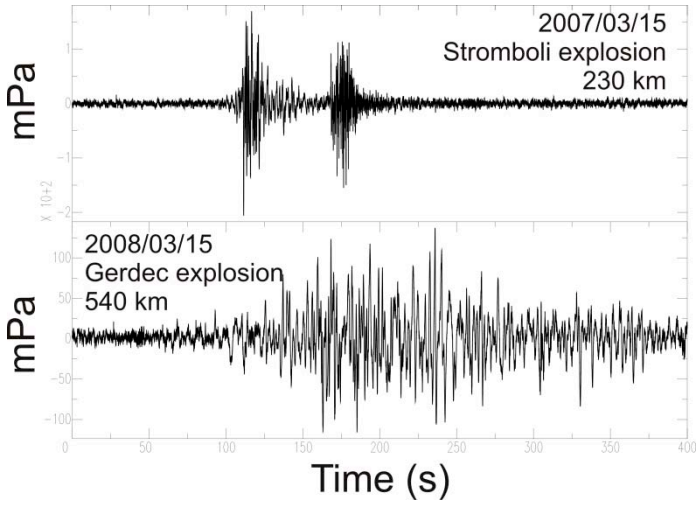

Figure 15. Signals of the two most significant regional events recorded since 2006. The distance of the CSFT station from the sources is indicated.

References

Arrowsmith S.J., Johnson J.B., Drob D.P., Hedlin M.A.H. (2010). The seismoacoustic wavefield: a new paradigm in studying geophysical phenomena. Rev. Geoph. Vol.48, RG4003.

Chaparral 25 V datasheet: http://www.chaparral.gi.alaska.edu/ChaparralModel25VManualr3.pdf.

D'Auria L., Marotta E., Martini M., Ricciolino P. (2006). Seismic and acoustic detection of a bolide airburst in the Gulf of Naples (southern Italy). J. Geoph. Res. Vol.111, B10307.

Evers L.G. and Haak W. (2009). The characteristics of infrasound, its propagation and some early history. In: Infrasound Monitoring for Atmospheric Studies (Le Pichon, Blanc, and Hauchecorne, ed.) pp. 141-182. Springer, Netherlands.

Martini M., et al. (2007) Seismological monitoring of the February 2007 effusive eruption of the Stromboli volcano. Ann. Geoph. Vol.50 No.6 pp.775-788.

Orazi M., Martini M. and Peluso R. (2006). Data acquisition for volcano monitoring. Eos vol.87, no.38, pp.385-382.

Sessler G. M. (1987). Electrets. Springer-Verlag, Berlin.

Shams Q.A., Zuckerwar A.J. and Sealey B.S (2005). Compact nonporous windscreen for infrasonic measurements. J. Acoust. Soc. Amer., 118(3), 1335-1340.

Walker K.T. and Hedlin M.A.H. (2009). A review of wind-noise reduction methodologies. In: Infrasound Monitoring for Atmospheric Studies (Le Pichon, Blanc, and Hauchecorne, ed.) pp. 141-182. Springer, Netherlands.

WM034 series datasheet (http://www.datasheetarchive.com/pdf-datasheets/Datasheets-24/DSA-475100.html).

Coordinamento editoriale e impaginazione
Centro Editoriale Nazionale | INGV

Progetto grafico e redazionale
Daniela Riposati | Laboratorio Grafica e Immagini | INGV

Via di Vigna Murata, 605
00143 Roma
Tel. +39 06518601 Fax +39 065041181

http://www.ingv.it

Istituto Nazionale di Geofisica e Vulcanologia